HHS Public Access

Author manuscript

Leukemia. Author manuscript; available in PMC 2015 September 01.

Published in final edited form as:

Leukemia. 2015 March ; 29(3): 556–566. doi:10.1038/leu.2014.241.

Augmented efficacy with the combination of blockade of the NOTCH-1 pathway, Bortezomib and Romidepsin in a murine MT-1 adult T cell leukemia model

Ping Yu[1], **Michael N. Petrus**[1], **Wei Ju**[1], **Meili Zhang**[1,2], **Kevin C. Conlon**[1], **Masao Nakagawa**[1], **Michiyuki Maeda**[3], **Richard N. Bamford**[4], and **Thomas A. Waldmann**[1]

[1]Lymphoid Malignancies Branch, Center for Cancer Research, National Cancer Institute, Bethesda, Maryland 20892, USA

[2]Laboratory Animal Science Program, SAIC-Frederick, Inc., NCI-Frederick, Frederick, Maryland, 21702

[3] Institute for Virus Research, Kyoto University, Sakyo-ku, Kyoto 606-8507, Japan

[4]Transponics, Jacobus, PA

Abstract

Adult T-cell leukemia (ATL) is an aggressive malignancy caused by human T-cell lymphotropic virus I (HTLV-1). There is no accepted curative therapy for ATL. We have reported that certain ATL patients have increased Notch-1 signaling along with constitutive activation of the NF-κB pathway. Physical and functional interaction between these two pathways provides the rationale to combine the γ-secretase inhibitor Compound E with the proteasome inhibitor Bortezomib. Moreover, Romidepsin, a histone deacetylase inhibitor, has demonstrated major antitumor action in leukemia/lymphoma. In this study, we investigated the therapeutic efficacy of the single agents and combinations of these agents in a murine model of human ATL, the MT-1 model. Single and double agents inhibited tumor growth as monitored by tumor size ($P < .05$), and prolonged survival of leukemia-bearing mice ($P < .05$) compared with the control group. The combination of three agents significantly enhanced the antitumor efficacy as assessed by tumor size, tumor markers in the serum (human sIL-2Rα and β_2M), and survival of the MT-1 tumor bearing mice, compared with all other treatment groups ($P < .05$). Improved therapeutic efficacy obtained by combining Compound E, Bortezomib and Romidepsin supports a clinical trial of this combination in the treatment of ATL.

Keywords

Adult T-cell leukemia; Notch-1; Bortezomib; Romidepsin

Corresponding author: Thomas A. Waldmann, M.D., Building 10, Room 4N115, 10 Center Drive, Bethesda, MD 20892-1374, TEL: (301) 496-6656, FAX: (301) 496-9956, tawald@mail.nih.gov.

Conflict-of-Interest: The authors report no conflicts-of-Interest.

Supplementary Information is available at Leukemia's website.

Introduction

Human HTLV-1-associated ATL is an aggressive leukemia/lymphoma of $CD3^{dim}CD4^{+}CD25^{+}$ T-cells[1,2]. HTLV-1-mediated T-cell transformation is a multistep oncogenic process in which virus induced chronic T-cell proliferation results in accumulations of genetic defects and dysregulated growth of infected cells. Of the 15–20 million HTLV-1 infected carriers worldwide, approximately 500,000 will ultimately develop ATL, a leukemia that is highly refractory to conventional therapy. Despite intensive efforts to improve the overall survival, ATL remains one of the hematologic malignancies with the poorest prognosis. At present, there is no accepted curative therapy for ATL, and patients with acute ATL have a median survival rate of 13 months[3]. The poor prognosis of ATL is mainly associated with its resistance to chemotherapy. Therefore, exploring novel innovative therapeutic strategies for ATL is critical.

ATL is typically preceded by decades of clinical latency during which HTLV-1 infected cells accumulate selectable traits leading to a malignant transformation. Although the precise mechanism is not completely understood, host pathways commandeered by the virus have provided therapeutic targets of benefit to patients. Constitutively activated Notch-1 and nuclear factor-κB(NF-κB) pathways have emerged as valuable targets in ATL.

Notch-1 is a single-transmembrane receptor composed of extracellular, transmembrane and intracellular subunits linked via heterodimerization domains[4,5]. Mammals have four Notch receptors(Notch1–Notch4), and five DSL ligands: Jagged1, Jagged2, Delta-like-1 (DLL-1), DLL-3 and DLL-4[6].Ligand binding induces proteolytic cleavage of receptor by several proteases(including γ-secretases), resulting in the release of an intracellular fragment of Notch-1(ICN-1), which translocates to the nucleus and activates the transcription of down-stream genes. Notch signaling is important in many developmental contexts and this is well exemplified by its role in cells of hematopoietic lineage[6]. Fifty percent of patients with acute T-lymphoblastic leukemia/lymphoma (T-ALL) have been demonstrated to carry activating mutations of Notch-1[7], and in our study we demonstrated activating PEST domain Notch-1 mutations in 40% of ATL patients[8]. The identification of Notch-1 as a potential oncogene in ATL opened the way for efforts to elucidate the signaling pathways involved in Notch-1-induced transformation.

NF-κB pathway is an important regulator of cell survival, cell cycle progression, cell adhesion and migration[9,10]. These processes, when deregulated, are the hallmarks of tumor induction. NF-κB pathway has been implicated in a variety of human cancers including the development of ATL. It has been demonstrated that T-cell transformation by HTLV-1 involves the deregulation and constitutive signaling of NF-κB[11-13]. These studies provide the scientific basis for targeting of NF-κB pathway in ATL.

Histone deacetylases(HDAC) are enzymes that remove acetyl groups from histones, resulting in the compaction of chromatin and the prevention of gene transcription. HDAC inhibitors reverse this process and induce apoptosis[14,15]. Romidepsin is a cyclin tetrapeptide HDAC inhibitor. In 2009, the Food and Drug Administration (FDA) granted approval for the treatment of cutaneous T-cell lymphoma(CTCL) patients with Romidepsin. Moreover,

Romidepsin has shown cytotoxic effects on malignant lymphoid cell lines, including HTLV-1–infected T-cell lines[16,17].

In the present study, using a murine ATL model (MT-1), we investigated the therapeutic efficacy of three reagents alone or in combination. Compound E was used as a γ-secretase inhibitor (GSI); Bortezomib as the proteasome inhibitor to block NF-κB activity and Romidepsin as an HDAC inhibitor. Each of three reagents alone or in double combination inhibited tumor growth as monitored by tumor size, the level of tumor markers in the serum, and significantly prolonged the survival of tumor-bearing animals($P<.05$). The combination of three reagents provided much greater therapeutic efficacy in the MT-1 ATL model and the median survival of tumor bearing animals was significantly prolonged when compared to all other treatment groups. Some of the triple combination treated animals had no detectable tumors at the end of study. Our data provides the scientific basis for the combination treatment of ATL patients with a γ-secretease inhibitor, Bortezomib and Romidepsin.

Materials and Methods

Drug

Compound E was obtained from Enzo life sciences, Inc(Farmingdale, NY, USA). Bortezomib, RO4929097 (another γ-secretease inhibitor) and Romidepsin were purchased from SelleckChemical.com(Houston, TX, USA).

Cells and inhibitory assay

Informed consent was obtained in accordance with the Declaration of Helsinki and was approved by the Investigational Review Board of National Cancer Institute (NCI). Peripheral blood mononuclear cells (PBMCs) were isolated from ATL patients by Ficoll-Hypaque. ATL subtypes were classified according to the diagnostic criteria proposed by Shimoyama et al[18]. ATL cell lines MT-1, ED40515(+)(ED+) , ED40515(−)(ED−), 43Tb−, LM-Y1, ED41214−, ST-1 as well as Hut-102(HTLV-1 infected cell line from a patient with ATL), Jurkat, HPB-ALL(T-ALL lines), Kit225(chronic T-cell-lymphocytic-leukemia) were used. The BJ fibroblast cell line and HCT-15 were used as controls. The inhibitory effects of inhibitors on cell growth were assayed by measuring [^{3}H]-thymidine incorporation. PBMCs from ATL patients were cultured *ex vivo* in the presence of inhibitors. On day 6 of the culture, ^{3}H-TdR was added for the last 6 hours. Cell proliferation was measured by thymidine incorporation. Detailed information is provided in SI Materials and Methods.

RT-PCR, sequencing and transfection

Q-PCR was performed with total RNA from MT-1 cells. The amplified PCR product was purified and was directly sequenced. Wild type human ICN-1 was transfected into 293T cells. Detailed information is provided in SI Materials and Methods.

Measurement of apoptotic cell death and caspase activity

For detection of apoptosis, Annexin-V-binding capacities of the treated cells were examined by flow cytometry using an Annexin-V-FITC/PI Apoptosis Detection Kit (eBioscience, San

Diego, CA, USA), according to the manufacture's instructions. For PBMCs from ATL patients, the percentages of specific apoptosis were calculated as follows: %specific apoptosis=(Annexin-V^+−spontaneous Annexin-V^+)/(100-spontaneous Annexin-V^+) ×100. The caspase-3 and caspase-9 activities were measured using caspase-3 and caspase-9 colorimetric assays from R&D Systems (Minneapolis, MN, USA).

Western blot analysis

Samples from whole-cell lysates were prepared and proteins (30μg) were subjected to Western blot analysis[8]. The blots were probed with antibodies to cleaved human Notch-1(Val 1744), and β-actin(Cell Signaling, Danvers, MA,USA).

siRNA transfections and cell viability analysis

MT-1 cells were transfected with Notch-1-siRNA and control-siRNA respectively, using siRNA transfection kits from Santa Cruz Biotechnology Inc(Santa Cruz, CA, USA) following manufacture's instructions. We determined changes in cell viability by Annexin-V-FITC/PI staining and analyzed by flow cytometry.

Cell cycle analysis

The cells were synchronized in G_0 by serum starvation for 24hs in phenol red–free-RPMI with 0.1% serum. Subsequently, cells were released into medium containing 10% FBS. Cells were fixed in 70% alcohol for 30 minutes at 4°C. Then cells were resuspended in PBS with PI and RNase-A for 30 minutes at 37°C. Samples were analyzed for DNA content using a FACSCalibur.

NF-κB transcription factor DNA-binding assays

To measure the activity of NF-κB pathway, levels of nuclear DNA-binding NF-κB subunits were assessed using TransAM NF-κB Family Kit (Active Motif). Fractionated protein lysates were prepared and the nuclear fractions were incubated on a 96-well plate containing immobilized NF-κB-consensus oligonucleotides. Bound NF-κB complexes were detected using specific antibodies directed against the different subunits, and quantified using a horseradish peroxidase-based colorimetric readout.

Mouse model of ATL

MT-1 cells(1×10^7) were subcutaneously injected into NOG(NOD/Shi-scid/IL-2Rγnull) mice to establish a tumor model. MT-1 cells have a characteristic ATL phenotype elucidated by flow cytometric analysis: $CD3^{dim}CD4^{+/-}CD25^+$. Therapeutic experiments were performed on selected mice with palpable tumors. All animal experiments were performed in accordance with NIH Animal Care and Use Committee guidelines.

Therapeutic study

Compound E was dissolved in polyethylene glycol-300(VWR Scientific Products, USA) at 10μmol/Kg, and continuously administered via a subcutaneous mini-osmotic pump (ALZET, CA, USA) for 28 days. Bortezomib was provided at 0.5mg/kg/injection by intraperitoneal injection twice weekly for 4 weeks. Romidepsin was administrated at

0.5mg/kg by i.p injection every other day for 4 weeks. One group of mice that received 200 μL PBS weekly for 4 weeks served as a control.

Monitoring tumor growth

Tumors were measured weekly, tumor size was calculated as mm^3=0.5×Length(mm) ×$Width^2$(mm). The measurements of the serum concentrations of soluble human IL-2Rα or β_2-microglobulin(β_2M) were performed using ELISA(R&D Systems, MN, USA) following manufacturer's recommendations.

Surface and intracellular staining of patients materials

Ficoll separated PBMCs from patients or healthy donors were incubated with APC-anti-CD4, PerCP-anti-CD3, PE-anti-CD25 plus antibodies against human Jagged-1, Jagged-2 or DLL-1 to detect the expression of Notch-1 ligands. Meanwhile, certain PBMCs were fixed with formaldehyde, then permeabilized by methanol and an intracellular staining was performed with antibodies against cleaved Notch-1(Val 1744), Jagged-1(H-114), Jagged-2(H-143) or DLL-1(H-265). All of the antibodies to detect ligands of Notch-1 were purchased from Santa Cruz Biotechnology Inc. Samples were then incubated with Alexa-Fluor-488 conjugated secondary antibodies. The expression of target molecules was detected by a FACSCalibur.

Statistical analysis

The differences in the tumor size of mice in each group were determined by ANOVA. Statistical significance of differences in survival of mice in different groups was determined by the log-rank test using JMP program(Abacus Concepts, Berkeley, CA, USA). Other data were analyzed using the Student's *t* tests.

Results

Constitutive activation of Notch-1 in HTLV-1–associated ATL cell lines

We previously reported that 40% of leukemia cells of ATL patients have activating Notch-1 mutations[8]. Initial studies were performed to examine the relative levels of Notch-1 in ATL cell lines. Among the five ATL cell lines assessed(MT-1, ED+, ED−, LM-Y1 and 43Tb−), increased expression of ICN-1 was only detected in MT-1 cells by Western Blot analysis(Figure 1A). Furthermore, direct sequencing of RT-PCR products of exon 34 demonstrated a missense mutation(C>T) at nucleotide position 7536 of the Notch-1 transcript. This results in a Pro 2513 Leu amino acid substitution in the C-terminal PEST domain of Notch-1(Figure 1B). PEST domain mutations in T-ALL led to increased levels of ICN-1 due to impaired degradation of activated receptor by proteasomes[7,19]. This is identical to the mutation found in several T-ALL lines and lies in a sequence that has been implicated in Fbw 7-mediated degradation of ICN-1[7, 20-21]. In MT-1 cells, wild type allele was not seen at nucleotide position 7536 suggesting that the cells had lost the other allele or perhaps are homogeneous for the trait. Additionally, subcloning and sequencing of exon 34 PCR genomic DNA products all demonstrated only the mutant allele. These data support the presence of an activating mutation in the Notch-1 gene in MT-1 cell line.

Treatment of MT-1 cell line with an inhibitor of the γ-secretase complex Compound E resulted in decreased expression of ICN-1, suggesting that in MT-1 cells, ICN-1 is produced mainly from normal receptor cleavage (Figure 1C). Additionally, increased cells apoptosis was observed in MT-1 cells transfected with Notch-1 siRNA compared to control siRNA, $P<0.05$(Figure 1D). Furthermore, we investigated the half-life of ICN-1 in MT-1 cells, normal PBMCs stimulated with DLL-4, and 293T cells transfected with Myc-tagged wild-type ICN-1 or mutated ICN-1 expression vectors used as controls. Cells were treated with cycloheximide for 3 or 6hs to prevent *de novo* protein synthesis. Western blot analyses confirmed reduced turnover of ICN-1 in MT-1 cells compared to normal PBMCs, similar to mutated ICN-1 compared to wild type ICN-1 expressed by transfected 293T cells (Fig 1E). Together, these data suggest that Notch-1 pathway is constitutively activated in MT-1 cells. Therefore, MT-1 cell line was chosen for further studies.

Compound E inhibited the proliferation and induced apoptosis in MT-1 cell lines

We examined the effects of Compound E and another γ-secretease inhibitor--RO4929097 on the proliferation of MT-1 cells. Various concentrations of inhibitors were used, and dose-dependent inhibition by Compound E addition was observed in MT-1 cells(Figure 2A). A similar pattern was shown in MT-1 by RO4929097 treatment (Figure 2B). However, other ATL cell lines(ED+, LM-Y1 and 43Tb−) that with no ICN-1 expression detected by Western blot were not affected by either of these inhibitors. Only modest suppression at high concentrations of Compound E was observed in ED− cells. This excludes off-target suppressive effects by Compound E and RO4929097. HPB-ALL cells were used as a positive control carrying an activated mutation of Notch-1[22]. Jurkat cells were used as a negative control, noting that a PTEN mutation makes these cells resistant to GSIs[23]. Staining of MT-1 cells with Annexin-V demonstrated that a significant proportion of cells had undergone apoptosis 48 hours after Compound E treatment (Figure 2C). Both caspase-9 and caspase-3 activities as measured by colorimetric assays were induced in the MT-1 cell line 24hs after Compound E treatment (Figure 2D).

Bortezomib treatment inhibited ATL cell proliferation and induced cell apoptosis/death

ATL cell lines were treated with various concentrations of Bortezomib for 48 hours. Bortezomib inhibited the proliferation of all tested ATL cell lines in a dose-dependent manner (Figure 3A). BJ human fibroblast cells were used as a control. Using Annexin-V staining we demonstrated that some MT-1 cells underwent apoptosis and cell death after Bortezomib treatment (Figure 3B). Both caspase-9 and caspase-3 activities were induced in ATL cell lines after 24 hours of Bortezomib treatment (Figure 3C, 3D).

Romidepsin treatment inhibited the proliferation of cells and induced cell cycle arrest

The inhibitory effect of Romidepsin on cell proliferation was evaluated by culturing ATL cells, as well as control cell lines (Jurkat, Hut-102 and HCT-15), with various concentrations (0-40nM) of Romidepsin for 6 hours. Dramatic suppression was observed in ATL cell lines (Figure 4A). Consistent with its effect on cell growth inhibition, Romidepsin induced cell cycle arrest significantly at the G_2/M phase in MT-1, 43Tb− and Jurkat cells (Figure 4B, 4C). Romidepsin treatment (4nM) for 24 h resulted in 32.43%, 35.39% and 44.19%

accumulation of cells in G_2/M phase in these three cell lines respectively. This suggests that there is a blockade in the G_2/M phase transition, which may induce the cells to undergo apoptosis/cell death. An increase in the sub-G_1 population also suggested the presence of apoptotic cells (Figure 4B, 4C). PI staining of treated MT-1 cells confirmed this mechanism, with an obvious population of PI^+ cells observed upon Romidepsin treatment (Figure 4D).

Additive/synergistic inhibitory effect on MT-1 cells by the combination of Compound E, Bortezomib and Romidepsin *in vitro*

We quantitatively analyzed the changes in DNA binding activity of the different NF-κB subunits after Compound E treatment in MT-1 cells(Figure 5A). Nuclear protein samples were prepared, and protein binding to NF-κB responsive DNA oligonucleotides was analyzed with TransAM NF-κB family kit (Active Motif). To confirm the specificity of the assay, two oligonucleotides were provided as a competitor for NF-kB binding. Wild-type consensus oligonucleotides prevented NF-kB binding to the probe immobilized on the plate. In contrast, the mutated consensus oligonucleotide had no effect on DNA binding (data not shown). Strong reduction of DNA binding activity was observed for the p52 and RelB subunits in MT-1 cells in a dose-dependent manner(Figure 5A). Modest inhibition of the p65 subunit was detected with low dose Compound E treatment (Figure 5A). No obvious suppression was detected on p50 or c-Rel. However, DNA binding activity for p50 and c-Rel subunits was reduced upon Bortezomib treatment in MT-1 cells (Figure 5B). When we combined Compound E with Bortezomib, they effectively inhibited the NF-kB pathway in MT-1 cells(Figure 5B). Our data support the view that Notch contributes to the regulation of alternative NF-κB signaling[24]. This suggests that in MT-1 cells, Notch inhibition exerts its biological effects at least in part through downregulation of alternative NF-κB signaling. Moreover, the co-operation of Bortezomib(1nM) with Romidepsin(2nM) effectively triggered the caspase pathway with increased caspase 3 and 9 activity even at low doses, as shown in Fig 5C, compared to each agent alone, $P<0.05$. Romidepsin(2nM) along with the combination of Compound E(1μM) and Bortezomib (1nM), significantly inhibited the proliferation of MT-1 cells as assessed by an *in vitro* assay(Figure 5D), when compared to that observed in single agent or double combination agents groups, $P<0.05$.

Effective treatment of ATL with Compound E, Bortezomib and Romidepsin in MT-1 *in vivo* murine model of human ATL

In the MT-1 model, a 4-week course of treatment with Compound E, Bortezomib, Romidepsin and the combination of these agents demonstrated therapeutic efficacy as assessed by both tumor growth(Figure 6A) and survival of tumor bearing mice(Figure 6B). Single agent and double combination treated groups had significantly smaller tumors and longer survival times compared to control group($P<.05$). Moreover, growth of tumors in the triple combination treatment group was reduced when compared to all other groups($P<0.05$). Prolonged survival times of tumor bearing animals in the triple combination treatment group was observed when compared to control group(mean survival: 85 vs. 36 days, $P=0.001$); Compound E alone group (median survival: 85 vs. 50 days; $P=0.025$); Bortezomib alone group(median survival: 85 vs. 44 days, $P=0.002$); Romidepsin alone group(median survival: 85 vs 47 days, $P=0.009$); Compound E + Bortezomib group(85 vs 53 days, $P=0.020$); Bortezomib+Romidepsin group(85 vs 55 days, $P=0.028$), and Compound E +

Romidepsin(85 vs 51 days, P=0.021). In the triple combination treatment group, 30-40% of the initially treated animals did not have detectable tumors at the study termination(100 days after tumor inoculation). Meanwhile, serum levels of human soluble IL-2Rα (CD25) and human β_2M also reflected the therapeutic efficacy(Figure 6C, 6D). Compared with serum concentrations of sIL-2Rα and β_2M in the control group at 5 weeks after tumor inoculation, there were reductions of sIL-2Rα and β_2M levels in triple combination treated animals(sIL-2Rα, 1422±130 vs 47608±9000 pg/ml, $P < 0.01$; β_2M, 130±46 vs 2000±465 ng/ml, P <0.01). Furthermore, although single agent and double combination treatment groups showed significant decreases in sIL-2Rα and β_2M, the triple combination therapy group demonstrated a far greater decrease in these markers.

Ex vivo ATL cells in PBMCs of ATL patients had increased ICN-1 expression and upregulated Notch-1 ligands expression

Intracellular staining was performed to detect ICN-1 protein levels in patients with chronic/smoldering ATL along with normal PBMCs as controls. Increased expression levels of ICN-1 were detected in patient ATL cells when compared to normal un-separated $CD4^+$ T-cells in PBMCs as shown by mean fluorescence intensity(MFI) in FACS analysis(Figure 7A). Meanwhile, it is well known that Notch ligand-induced extracellular cleavage regulates the activation of Notch-1[6]. After gating on $CD3^{low}CD4^{high}$ cells, increased surface expressions of Notch ligands--Jagged 1, Jagged 2 and DLL-1 were detected in ATL-2 patient compared to normal PBMCs by flow cytometry(Figure 7B). Among all ATL patients, increased surface expression of Jagged-1 (MFI=26.9±10.1), and Jagged-2(MFI=29.9±14.2) were detected, compared to normal and ICN^{low} groups, P<0.05. Meanwhile, intracellular expression levels of all three ligands were upregulated in the ICN^{high} group, with Jagged-1(MFI=123.5±31.9), Jagged-2(MFI=190±52.5) and DLL-1(MFI=185.9±42.2), compared to ICN-1^{low} group and the normal donors group, P<0.05(Figure 7C, 7D).

Ex vivo triple combination treatment induced early apoptosis of PBMCs of ATL cells from patients with increased ICN-1 expression

Ex vivo apoptosis assays of PBMCs in chronic/smoldering ATL patients with increased ICN-1 expression were performed by treating PBMCs with inhibitors. Apoptosis was determined by flow cytometric analysis using Annexin-V-FITC/PI staining. The percentage of early-apoptotic cells was measured by defining the percentage of the Annexin-V^+PI^- cells after incubation with the indicated reagents(Figure 8A). Statistical analysis suggested that the triple combination treatment significantly increased early apoptosis cells when compared to all single or double combination groups, P<.01(Figure 8B). Moreover, the spontaneous proliferation observed with PBMCs from eight patients was inhibited by the addition of Compound E, Bortezomib and Romidepsin(Figure 8C). Statistical analysis suggested that the triple combination treatment significantly inhibited 6-day ex vivo spontaneous cell proliferation when compared to other single or double combination groups (Figure 8C). Compared to normal donors and patients with low ICN-1 expression group (Supplementary Figure 1, 2), these data reflect the underlying correlation between increased ICN-1 expression and the response to Compound E, Bortezomib and Romidepsin triple combination treatments.

Discussion

Currently, there is no effective curative therapy for patients with HTLV-1–associated ATL. A number of strategies such as chemotherapy and anti-retroviral agents have been evaluated for the treatment of ATL patients without significant curative benefit. So far there is no standard therapy for the majority of ATL patients. Given the limitations in treatment for these patients, newer therapeutic strategies are required.

Studies on T-ALL have suggested that Notch-1 is an important molecular target in this disease[25], since half of the T-ALL patients have activating mutations in Notch-1[7, 26]. Whereas significant numbers of HTLV-1- associated ATL patients have Notch-1 mutations[8], the current therapeutic strategies have not included regimens targeting the Notch-1 signaling pathway.

Currently, in some of our chronic/smoldering ATL patients we have detected increased Notch-1 signal in the leukemic cells compared to un-separated normal $CD4^+$ T-cells in PBMCs by observing increased ICN-1 expression (Fig 7A). In addition, we demonstrated that the spontaneous proliferation of PBMCs could be inhibited by addition of Compound E(Fig. 8C). These observations provide the scientific basis for the application of this inhibitor in the clinic for the treatment of patients with ATL. Meanwhile, Notch signaling is proving increasingly complex and it appears to be integrated with other pathways in normal and abnormal circumstances. There are reciprocal transcriptional regulations between Notch and NF-κB[27]. Specifically, Notch-1 has been reported to strongly induce NF-κB2 promoter activity in reporter assays[28]. In T-ALL, ICN-1 expression induced the nuclear localization of NF-κB, which resulted in the expression of multiple NF-κB targets (including Bcl-2A1, NF-κB2 and ICAM1) [22, 29-30]. These observations offer a complex picture of the interactions between these two pathways. Therefore, when we focus on the manipulation of the Notch-signaling pathway for experimental or therapeutic purposes, it will be important to pay attention to the possible effects of Notch-1 manipulation on NF-κB and vice versa. This is especially true with certain ATL patients who have increased Notch-1 signaling along with up-regulated NF-κB activity. Treatments inhibiting both pathways may be complementary.

Currently in MT-1 cells, both canonical and non-canonical pathways exist and contribute to the constitutive NF-κB activity[31]. Vilimas T et al.[32] reported that ICN-1 activated the NF-κB pathway by interacting with the IKK complex and by increasing transcription of NF-κB2 and Rel B. This was confirmed in our study: when low doses of Compound E were provided to MT-1 cells, decreased DNA binding activity of p52 and Rel B was observed(Fig 5A, 5B). Meanwhile, with Bortezomib, a proteasome inhibitor, potent inhibition of the growth of ATL cells both *in vivo* and *in vitro* was observed. The underlying mechanism was suggested to be by increased phosphorylation of IκBα protein in both cell lines and primary ATL cells[33]. This provided the scientific rational for our combination of low doses of Bortezomib and Compound E, that resulted in inhibition of DNA binding activity of all five subunits of the NF-κB pathway(Fig 5B). Furthermore, we obtained significantly increased cytotoxic activity with the combination when compared to either agent alone *in vitro* and *in vivo* (Figure 5D,6). This observation is consistent with the reported additive/synergistic functions between GSIs and Bortezomib[34]. With the presence of increased Notch-1 signaling in some

ATL patients, combination of low dose of GSI with Bortezomib may lead to increased efficacy without serious toxicity.

Romidepsin belongs to the cyclic peptide class of HDAC inhibitors and is currently undergoing clinical trials as a treatment for CTCL, peripheral T-cell lymphoma, and a variety of other cancers. Upon Romidepsin treatment, significant apoptosis was induced in HTLV-1–infected T-cell lines[16]. More importantly, it was reported in various disease models, including multiple myeloma and mantle cell lymphoma, that there is synergy between Bortezomib and HDAC inhibitors [35-37]. In chronic lymphocytic leukemia(CLL) Bortezomib blocked Romidepsin-mediated RelA acetylation, prevented Romidepsin from induction of NF-κB activation, and the *de novo* expression of its target gene IκBα. Moreover, this combination triggered a cell apoptosis pathway, reflected by caspase activation, and finally led to cell death of both primary CLL and cell lines[38]. Currently, whereas exposure to low doses of each agent alone resulted in slight increases of caspase-3 and caspase-9 in MT-1 cells; the combined treatment resulted in a clear increase in activation of caspase-3 and caspase-9, and cell death (Fig 5C,5D). In addition the combination of Bortezomib with Romidepsin provided more pronounced cytotoxic activity than either agent alone in both an animal model and with patients *ex vivo* PBMCs (Figures 6 and 8).

The Notch-1 signaling pathway is initiated upon ligand binding and the Notch-1 receptor is cleaved by the γ-secretase complex and the released ICN-1. DLL-1 and Jagged-1 are processed in a fashion similar to Notch-1, ultimately resulting in the release of a nuclear-targeted intracellular domain[39-40]. More importantly, Delta ligand was shown to be co-localized with the extra-cellular domain of Notch(NECD), which means NECD forms a complex with Delta. This is critical for Notch activation and is required to achieve processing and dissociation of the Notch protein. Thus subsequent Notch signaling is dependent on Delta endocytosis and NECD trans-endocytosis[41]. Intriguingly, it has been reported that Jurkat cells, primary Hodgkin Reed-Sternberg cells and anaplastic large cell lymphoma(ALCL) cells express both Notch-1 and Jagged-1[42,43]. Both DLL-1 and Jagged-1 have been detected in glioma cell lines and primary human gliomas[44]. Furthermore, studies have shown that in B-ALL cells that expressed all Notch receptors and ligands, the reciprocal cell interactions via Notch signaling played an important role in the leukemia cell survival[45]. Currently, we observed increases in both surface and intracellular expressions of Notch-1 ligands in some ATL leukemia cells along with upregulated ICN-1 expression.

Previous studies on T-ALL focused on the activating mutations of Notch-1. Recently, researchers have suggested that the induction of T cell leukemia is dependent on the signaling strength of Notch-1 and that the signal strengths of the more common Notch-1 mutation alleles are insufficient to induce T-ALL on their own. Thus Notch-1 mutations appear to be additional events that can cooperate with oncogenic hits and thereby influence tumor development and onset[24]. Importantly, these tumors seem to remain “addicted” to Notch-1 signaling[46], which justified further exploration of notch inhibitors in the treatment of T cell leukemia. In our current study, among 14 ATL patients, only ATL-4 was shown to carry a Notch-1 mutation (Table-1, ATL-21)[8]. This different incidence from our previous report might be due to the different set of patients studied, which in the present case was

predominantly at the early stage of smoldering/chronic ATL. Nevertheless 8 of 14 were shown to highly express ICN-1. Furthermore, after gating on $CD3^{low}CD4^{high}$ T-cells, there was significantly increased expression of Notch-1 ligands in the ICN-1^{high} ATL patient group detected by both surface and intracellular staining(Fig 7B-D). Thus it appears that Notch-1 signaling can be activated by its ligands expressed in ATL leukemia cells through homotypic or heterotypic cell-cell interactions, thereby providing an autocrine or reciprocal activation of Notch-1 signaling among the ATL leukemia cells that favor their own survival.

In summary, the functional interactions between Notch and NF-κB provide the scientific basis for a rational drug combination therapy. The co-activation of Notch-1 and NF-κB exists in select ATL patients thereby providing a valuable rational for the application of a combination therapeutic strategy. Our results support the clinical development of a combination therapy that includes a γ-secretase inhibitor which might serve as an effective therapeutic agent in patients with chronic/smoldering ATL whose cells express increased Notch-1 signaling. In conclusion, our data demonstrated that one of the GSIs --- Compound E had antitumor activity both *in vitro* and *in vivo*. Furthermore, combination therapy of Compound E, Bortezomib with Romidepsin had significantly greater therapeutic effects in the MT-1 murine model of ATL than any single agent alone or any of the pairs of agents. The results of our study support a trial of GSI in ATL patients, preferably as an agent in combination with Bortezomib and Romidepsin.

Supplementary Material

Refer to Web version on PubMed Central for supplementary material.

Acknowledgement

This work was supported by the Intramural Research Program of Center for Cancer Research, NCI, NIH.

References

1. Hinuma Y, Nagata K, Hanaoka M, Nakai M, Matsumoto T, Kinoshita KI, et al. Adult T-cell leukemia: antigen in an ATL cell line and detection of antibodies to the antigen in human sera. Proc Natl Acad Sci U S A. 1981; 78:6476–6480. [PubMed: 7031654]
2. Poiesz BJ, Ruscetti FW, Gazdar AF, Bunn PA, Minna JD, Gallo RC. Detection and isolation of type C retrovirus particles from fresh and cultured lymphocytes of a patient with cutaneous T-cell lymphoma. Proc Natl Acad Sci U S A. 1980; 77:7415–7419. [PubMed: 6261256]
3. Yamada Y, Tomonaga M, Fukuda H, Hanada S, Utsunomiya A, Tara M, et al. A new G-CSF-supported combination chemotherapy, LSG15, for adult T-cell leukaemia-lymphoma: Japan Clinical Oncology Group Study 9303. Br J Haematol. 2001; 113:375–382. [PubMed: 11380402]
4. Vacca A, Felli MP, Palermo R, Di Mario G, Calce A, Di Giovine M, et al. Notch3 and pre-TCR interaction unveils distinct NF-kappaB pathways in T-cell development and leukemia. EMBO J. 2006; 25:1000–1008. [PubMed: 16498412]
5. Wilson JJ, Kovall RA. Crystal structure of the CSL-Notch-Mastermind ternary complex bound to DNA. Cell. 2006; 124:985–996. [PubMed: 16530045]
6. Radtke F, Schweisguth F, Pear W. The Notch 'gospel'. EMBO Rep. 2005; 6:1120–1125. [PubMed: 16299468]
7. Weng AP, Ferrando AA, Lee W, Morris JP 4th, Silverman LB, Sanchez-Irizarry C, et al. Activating mutations of NOTCH1 in human T cell acute lymphoblastic leukemia. Science. 2004; 306:269–271. [PubMed: 15472075]

8. Pancewicz J, Taylor JM, Datta A, Baydoun HH, Waldmann TA, Hermine O, et al. Notch signaling contributes to proliferation and tumor formation of human T-cell leukemia virus type 1-associated adult T-cell leukemia. Proc Natl Acad Sci U S A. 2010; 107:16619–16624. [PubMed: 20823234]
9. Karin M, Greten FR. NF-kappaB: linking inflammation and immunity to cancer development and progression. Nat Rev Immunol. 2005; 5:749–759. [PubMed: 16175180]
10. Karin M. Nuclear factor-kappaB in cancer development and progression. Nature. 2006; 441:431–436. [PubMed: 16724054]
11. Portis T, Harding JC, Ratner L. The contribution of NF-kappaB activity to spontaneous proliferation and resistance to apoptosis in human T-cell leukemia virus type 1 Tax-induced tumors. Blood. 2001; 98:1200–1208. [PubMed: 11493471]
12. Peloponese J, Yeung M, Jeang K-T. Modulation of nuclear factor-kB by human T-cell leukemia virus type 1 tax protein: Implications for oncogenesis and inflammation. Immunol Res. 2006; 34:1–12. [PubMed: 16720895]
13. Horie R. NF-kappaB in pathogenesis and treatment of adult T-cell leukemia/lymphoma. Int. Rev. Immunol. 2007; 26:269–281. [PubMed: 18027201]
14. Marks PA, Rifkind RA, Richon VM, Breslow R, Miller T, Kelly WK. Histone deacetylases and cancer: causes and therapies. Nat Rev Cancer. 2001; 1:194–202. [PubMed: 11902574]
15. Piekarz RL, Frye R, Prince HM, Kirschbaum MH, Zain J, Allen SL, et al. Phase 2 trial of romidepsin in patients with peripheral T-cell lymphoma. Blood. 2011; 117:5827–5834. [PubMed: 21355097]
16. Marks PA, Richon VM, Rifkind RA. Histone deacetylase inhibitors: inducers of differentiation or apoptosis of transformed cells. J Natl Cancer Inst. 2000; 92(15):1210–1216. [PubMed: 10922406]
17. Mori N, Matsuda T, Tadano M, Kinjo T, Yamada Y, Tsukasaki K, et al. Apoptosis induced by the histone deacetylase inhibitor FR901228 in human T-cell leukemia virus type 1-infected T-cell line and primary adult T-cell leukemia cells. J Virol. 2004; 78:4582–4590. [PubMed: 15078940]
18. Shimoyama M. Diagnostic criteria and classification of clinical subtypes of adult T-cell leukemia-lymphoma. Br J Haematol. 1991; 79:428–437. [PubMed: 1751370]
19. Thompson BJ, Buonamici S, Sulis ML, Palomero T, Vilimas T, Basso G, et al. The SCFFBW7 ubiquitin ligase complex as a tumor suppressor in T cell leukemia. J Exp Med. 2007; 204:1825–1835. [PubMed: 17646408]
20. O'Neil J, Grim J, Strack P, Rao S, Tibbitts D, Winter C, et al. FBW7 mutations in leukemic cells mediate NOTCH pathway activation and resistance to gamma-secretase inhibitors. J Exp Med. 2007; 204:1813–1824. [PubMed: 17646409]
21. Agnusdei V, Minuzzo S, Frasson C, Grassi A, Axelrod F, Satyal S, et al. Therapeutic antibody targeting of Notch1 in T-acute lymphoblastic leukemia xenografts. Leukemia. 2014; 28:278–288. [PubMed: 23774673]
22. Zuurbier L, Homminga I, Calvert V, te Winkel ML, Buijs-Gladdines JG, Kooi C, et al. NOTCH1 and/or FBXW7 mutations predict for initial good prednisone response but not for improved outcome in pediatric T-cell acute lymphoblastic leukemia patients treated on DCOG or COALL protocols. Leukemia. 2010; 24:2014–22. [PubMed: 20861909]
23. Palomero T, Sulis ML, Cortina M, Real PJ, Barnes K, Ciofani M, et al. Mutational loss of PTEN induces resistance to NOTCH1 inhibition in T-cell leukemia. Nat Med. 2007; 13:1203–1210. [PubMed: 17873882]
24. Schwarzer R, Dörken B, Jundt F. Notch is an essential upstream regulator of NF-κB and is relevant for survival of Hodgkin and Reed-Sternberg cells. Leukemia. 2012; 26:806–813. [PubMed: 21946908]
25. Sanda T, Li X, Gutierrez A, Ahn Y, Neuberg DS, O'Neil J, et al. Interconnecting molecular pathways in the pathogenesis and drug sensitivity of T-cell acute lymphoblastic leukemia. Blood. 2010; 115:1735–1745. [PubMed: 20007543]
26. Grabher C, von Boehmer H, Look AT. Notch 1 activation in the molecular pathogenesis of T-cell acute lymphoblastic leukaemia. Nat Rev Cancer. 2006; 6(5):347–359. [PubMed: 16612405]
27. Osipo C, Golde TE, Osborne BA, Miele LA. Off the beaten pathway: the complex cross talk between Notch and NF-kappaB. Lab Invest. 2008; 88(1):11–17. [PubMed: 18059366]

28. Oswald F, Liptay S, Adler G, Schmid RM. NF-κB2 Is a Putative Target Gene of Activated NOTCH-1 via RBP-Jκ. Mol Cell Biol. 1998; 18(4):2077–2088. [PubMed: 9528780]
29. Bellavia D, Campese AF, Alesse E, Vacca A, Felli MP, Balestri A, et al. Constitutive activation of NF-kB and T-cell leukemia/lymphoma in Notch3 transgenic mice. EMBO J. 2000; 19:3337–3348. [PubMed: 10880446]
30. Guan E, Wang J, Laborda J, Norcross M, Baeuerle PA, Hoffman T. T cell leukemia-associated human Notch/translocation-associated Notch homologue has IkB-like activity and physically interacts with nuclear factor-kB proteins in T cells. J Exp Med. 1996; 183:2025–2032. [PubMed: 8642313]
31. Hironaka N, Mochida K, Mori N, Maeda M, Yamamoto N, Yamaoka S. Tax-independent constitutive IkappaB kinase activation in adult T-cell leukemia cells. Neoplasia. 2004; 6:266–78. [PubMed: 15153339]
32. Vilimas T, Mascarenhas J, Palomero T, Mandal M, Buonamici S, Meng F, et al. Targeting the NF-kappaB signaling pathway in Notch1-induced T-cell leukemia. Nat Med. 2007; 13:70–77. [PubMed: 17173050]
33. Satou Y, Nosaka K, Koya Y, Yasunaga JI, Toyokuni S, Matsuoka M. Proteasome inhibitor, bortezomib, potently inhibits the growth of adult T-cell leukemia cells both in vivo and in vitro. Leukemia. 2004; 18:1357–63. [PubMed: 15190257]
34. Chen F, Pisklakova A, Li M, Baz R, Sullivan DM, Nefedova Y. Gamma-secretase inhibitor enhances the cytotoxic effect of bortezomib in multiple myeloma. Cell Oncol (Dordr). 2011; 34:545–551. [PubMed: 21965140]
35. Kikuchi J, Wada T, Shimizu R, Izumi T, Akutsu M, Mitsunaga K, et al. Histone deacetylases are critical targets of bortezomib-induced cytotoxicity in multiple myeloma. Blood. 2010; 116:406–417. [PubMed: 20351311]
36. Harrison SJ, Quach H, Link E, Seymour JF, Ritchie DS, Ruell S, et al. A high rate of durable responses with romidepsin, bortezomib, and dexamethasone in relapsed or refractory multiple myeloma. Blood. 2011; 118:6274–6283. [PubMed: 21911830]
37. Paoluzzi L, Scotto L, Marchi E, Zain J, Seshan VE, O'Connor OA. Romidepsin and Belinostat Synergize the Antineoplastic Effect of Bortezomib in Mantle Cell Lymphoma. Clin Cancer Res. 2010; 16:554–565. [PubMed: 20068080]
38. Dai Y, Chen S, Kramer LB, Funk VL, Dent P, Grant S. Interactions between bortezomib and romidepsin and belinostat in chronic lymphocytic leukemia cells. Clin Cancer Res. 2008; 14:549–558. [PubMed: 18223231]
39. LaVoie MJ, Selkoe DJ. The notch ligands, Jagged and Delta, are sequentially processed by α-secretase and presenilin/γ-secretase and release signaling fragments. J Biol Chem. 2003; 278:34427–34437. [PubMed: 12826675]
40. Bland CE, Kimberly P, Rand MD. Notch-induced proteolysis and nuclear localization of the Delta ligand. J Biol Chem. 2003; 278:13607–13610. [PubMed: 12591935]
41. Parks AL, Klueg KM, Stout JR, Muskavitch MA. Ligand endocytosis drives receptor dissociation and activation in the Notch pathway. Development. 2000; 127:1373–1385. [PubMed: 10704384]
42. Yuan Y, Lu X, Chen X, Shao HW, Huang SL. Jagged 1 contributes to the drug resistance of Jurkat cells in contact with human umbilical cord-derived mesenchymal stem cells. Onco Lett. 2013; 6:1000–1016.
43. Jundt F, Anagnostopoulos I, Förster R, Mathas S, Stein H, Dörken B. Activated Notch1 signaling promotes tumor cell proliferation and survival in Hodgkin and anaplastic large cell lymphoma. Blood. 2002; 99:3398–4303. [PubMed: 11964309]
44. Purow BW, Haque RM, Noel MW, Su Q, Burdick MJ, Lee J, et al. Expression of Notch-1 and its ligands, Delta-like-1 and Jagged-1, is critical for glioma cell survival and proliferation. Cancer Res. 2005; 65:2353–2363. [PubMed: 15781650]
45. Nwabo Kamdje AH, Mosna F, Bifari F, Lisi V, Bassi G, Malpeli G, et al. Notch-3 and Notch-4 signaling rescue from apoptosis human B-ALL cells in contact with human bone marrow-derived mesenchymal stromal cells. Blood. 2011; 118:380–389. [PubMed: 21602525]

46. Chiang MY, Xu L, Shestova O, Histen G, L'heureux S, Romany C, et al. Leukemia-associated NOTCH1 alleles are weak tumor initiators but accelerate K-ras-initiated leukemia. J Clin Invest. 2008; 118:3181–3194. [PubMed: 18677410]

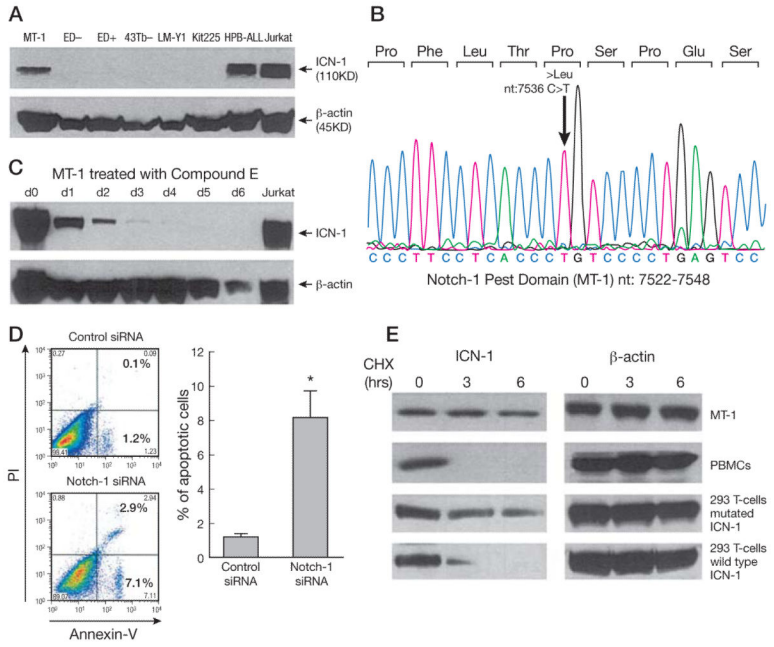

Figure 1. MT-1 cells have an increased expression of ICN-1 and the resultant activated pathway was inhibited by Compound E treatment in vitro

(A) Assay of expression of a cleaved form of Notch-1 (ICN-1) in ATL cell lines. Non HTLV-1 infected T-cell leukemia cell lines Kit225 (negative control), Jurkat (positive control) and HPB-ALL (positive control) cell lines were used as controls. The housekeeping gene beta-actin was used as a loading control. (B) The chromatogram of the Notch-1 PEST domain point mutation in MT-1 cells. (C) The expression of ICN-1 in MT-1 cells was inhibited by addition of Compound E. MT-1 cells were incubated with 1μM Compound E for various days. Total cell lysate (30μg/lane) was separated on sodium dodecyl sulfate-polyacrylamide gels, transferred to the membrane, and ICN-1 was detected by a Western blot with specific antibodies. Jurkat cells were used as a positive control. (D) The effect of siRNA-Notch-1 on MT-1 cells was assessed on the cell viability by Annexin-V-FITC/PI staining and analyzed by flow cytometry. MT-1 cells were treated with siRNA-Notch-1 or control siRNA. Data shown are representative of three independent experiments. The summary is shown in bar graph. **P*<0.05 compare to control siRNA group. (E) The half-life of ICN-1 was measured by a Western blot in MT-1 cells. Normal PBMCs stimulated with recombinant human Delta like ligand 4 (DLL-4, 5 μg/ml) overnight and 293T cells transfected with a Myc-tagged wild-type or mutated ICN-1 expression vector were used as controls. Cells were treated with cycloheximide (100μg/mL) for 0, 3, and 6 h. Beta-actin is shown as a loading control.

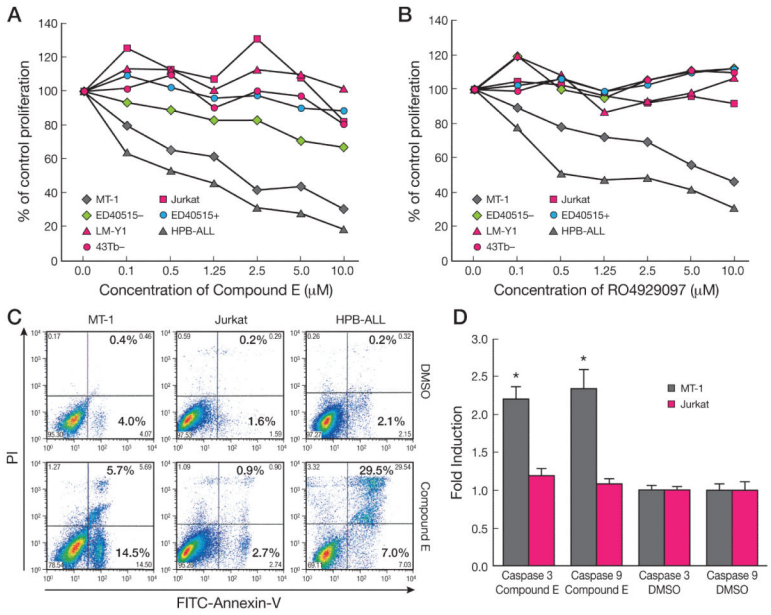

Figure 2. Compound E treatment inhibited ATL cell proliferation and induced apoptosis in MT-1 cells

(A) Compound E suppressed MT-1 cell proliferation in vitro. The cells were treated with various concentrations of Compound E (0, 0.1, 0.5, 1.25, 2.5, 5 or 10μM). The cell proliferation was measured 48 hours later by ^{3}H-thymidine incorporation. The data are shown as a percentage of that observed in untreated controls, and are representative of 3 independent experiments. MT-1 (grey diamonds), ED40515− (green diamonds), LM-Y1 (red triangles), 43Tb−(red dots), Jurkat (red squares), ED40515+ (blue dots) and HPB-ALL (grey triangles). (B) RO4929097 suppressed MT-1 cell proliferation in vitro. The data are shown as a percentage of untreated controls, and are representative of 3 independent experiments. (C) Induction of apoptosis by Compound E. The cells were treated with Compound E (10μM) or an equal volume of DMSO for 48 hours, and the apoptotic cells were measured by Annexin V/PI staining. HPB-ALL cells were used as a positive control, and Jurkat cells were used as a negative control. Data represent three independent experiments. (D) Induction of caspase-3 and caspase-9 activities by Compound E (5μM) in MT-1 cells. Jurkat cells were used as a control. The data are representative of 3 independent experiments (*P<0.05 compare to DMSO group).

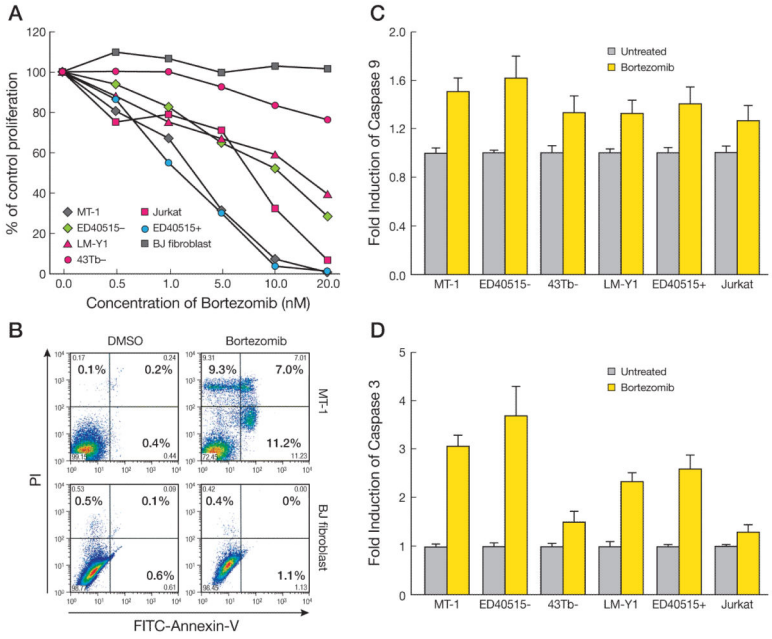

Figure 3. Bortezomib treatment inhibited cell line proliferation and induced cell apoptosis

(A) The cells were treated with various concentrations of Bortezomib (0, 0.5, 1, 5, 10, or 20nM), and the cell proliferation was measured 48 hours later by ^{3}H-thymidine incorporation. BJ human fibroblast cells were used as controls. The data are shown as percentage of untreated control, and are representative of three independent experiments. MT-1 (grey diamonds), ED40515− (green diamonds), LM-Y1 (red triangles), 43Tb− (red circles), Jurkat (red squares), ED40515+ (blue circles), and BJ fibroblast (grey squares). (B) Induction of MT-1 cell apoptosis by Bortezomib. MT-1 cells were treated with Bortezomib (5nM) or an equal volume of DMSO for 24 hours, and the cell apoptosis was measured by Annexin-V/PI staining. BJ human fibroblast cells were used as controls. The data represent three independent experiments. (C) Induction of caspase-9 activities by Bortezomib (5nM) was assessed. The data are representative of mean values from three independent experiments. (D) Induction of caspase-3 activities by Bortezomib (5nM). The data are representative of mean values of three independent experiments

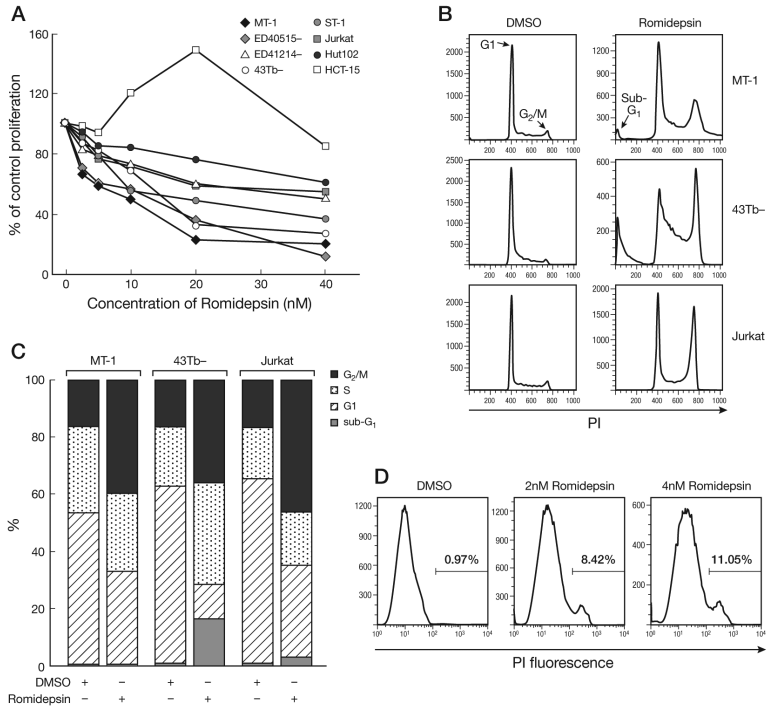

Figure 4. Inhibition of cell proliferation and cell cycle arrest was observed upon Romidepsin treatment

(A) MT-1 and all other cell lines were treated with variable concentrations of Romidepsin for 6 hours, then the inhibitor was washed out and the culture was continued with media for 42 hours. ^{3}H-TdR was added in the last 6h to quantitate cell proliferation. The data are shown as a percentage of untreated controls, and are representative of three independent experiments. MT-1 (black diamonds), ED40515− (grey diamonds), ED41214− (open triangles), 43Tb− (open dots), ST-1 (grey dots), Jurkat (grey squares), Hut 102 (black dots) and HCT-15 (open squares). (B) Effect of Romidepsin was assessed on cell cycle distribution in MT-1, 43Tb− and Jurkat cells. Cells were treated with Romidepsin (2nM) for 24 h. The percentages of cell cycle distributions were then evaluated by PI staining and flow cytometric analysis. Representative FACS histograms of cell cycle distribution are shown and labeled. (C) Cell cycle analyses are presented. Each column is representative of four repeat experiments. (D) Cell death induction by Romidepsin in MT-1 cells. MT-1 cells were treated with variable concentrations of Romidespin for 24 hours and cells were stained with PI. Gated cells represent dead cells stained brightly with PI. Data shown are representative of three independent experiments.

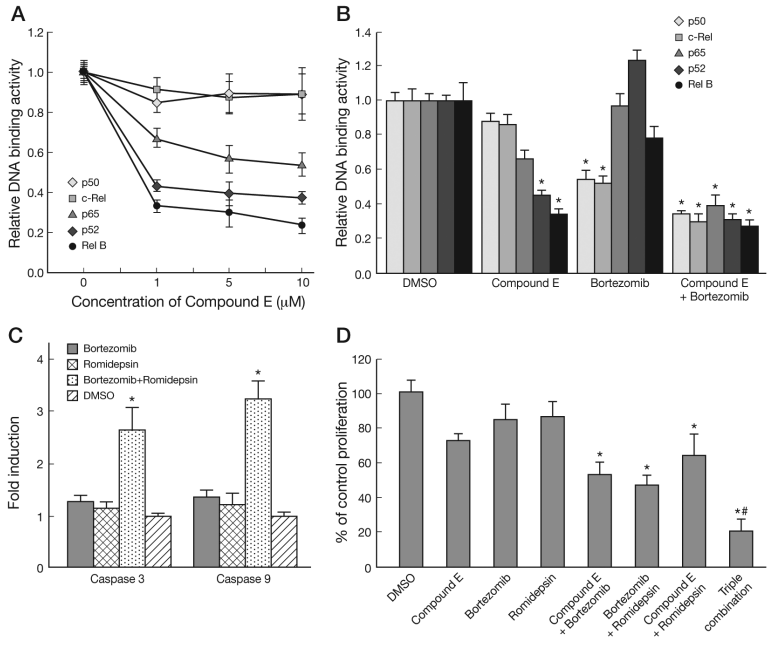

Figure 5. Additive/synergistic inhibitory effects on MT-1 cells by the combination of Compound E, Bortezomib and Romidepsin *in vitro*

(A) Compound E suppressed the DNA binding activities of p52 and Rel B. Nuclear extracts (5μg per sample) from MT-1 cells treated with different concentrations of Compound E were analyzed using a TransAM NF-kB transcription factor assay kit (Active Motif), according to the manufacturer's instructions. (B) The combination of Bortezomib with Compound E decreased DNA binding activities of all subunits of the NF-kB pathway. MT-1 cells were treated with 2nM Bortezomib with or without 1μM Compound E. Then nuclear extracts (5μg per sample) from treated cells were analyzed using the above kit (**P*<0.05 compared to DMSO group). (C) Increased inductions of caspase-9 and caspase 3 activities were observed with Bortezomib combined with Romidepsin in MT-1 cells. Bortezomib(1nM) with or without Romidepsin (2nM) was provided to MT-1 cells(**P*<0.05 compared to DMSO and single agent groups). (D) Additive/synergistic inhibitory effects were observed with MT-1 cells by the addition of a combination of Compound E, Bortezomib and Romidepsin *in vitro*. MT-1 cells were treated with Compound E (1μM), Bortezomib (2nM), Romidepsin (2nM) alone, or in double or triple combinations. The cell proliferation was measured 48 hours later by ^{3}H-thymidine incorporation. The data are shown as a percentage of untreated controls. A to D are representative of 3 independent experiments (**P*<0.05 compared to DMSO and single agent groups, # *P*<0.05 compared to double agents groups).

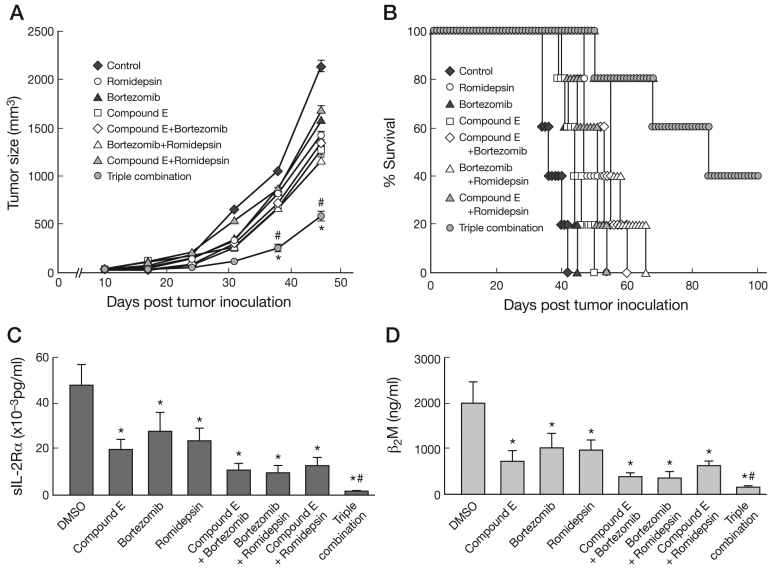

Figure 6. Triple combination of agents effectively prolonged the survival of MT-1 leukemia-bearing NOG mice

(A) 10 days after MT-1 tumor inoculation, mice with palpable tumors received diverse treatments. Compound E (10μmol/Kg) was provided consistently by osmotic pumps for four weeks, Bortezomib was intraperitoneally injected at 0.5mg/kg twice a week for four weeks. Romidepsin was administrated i.p every other day (0.5mg/kg) for four weeks. Selected animals received a combination treatment that included two or all three agents at the same dosage schedules. One group receiving PBS was used as a control. Growth curves illustrate *in vivo* growth rates of MT-1 tumors associated with diverse treatments. Tumor sizes shown represent Means ± SEM, n = 10 for each group (* $P<0.05$ compared to the control group; # $P<0.05$ triple combination group compared to one agent or two agent treatment groups). The data shown are representative of two independent experiments. Control (filled black diamonds), Romidepsin (open dots), Bortezomib (filled black triangles), Compound E (open squares), Compound E+Bortezomib (open diamonds), Bortezomib+Romidepsin (open triangles), Compound E+Romidepsin (grey triangles) and Triple Combination (grey circles). (B) Kaplan-Meier survival curves illustrate survivals of mice with diverse treatments. The animals treated with the Compound E, Bortezomib or Romidepsin alone or double combination groups as indicated in A had significantly prolonged survivals compared with the control group ($P< 0.05$). The triple combination treatment significantly prolonged the survival of leukemia-bearing mice compared with that of the control group ($P=0.001$), Compound E alone ($P =0.025$), Bortezomib alone ($P =0.002$) or Romidepsin alone ($P=0.009$); Compound E + Bortezomib group ($P=0.020$); Bortezomib+Romidepsin group ($P=0.028$), and Compound E + Romidepsin ($P=0.021$) Data shown are representative of two independent experiments. (C) The mean concentrations of human sIL-2R-α in picograms per milliliter in each group 5 weeks after tumor inoculation. (D) The mean concentrations of human β2M in nanograms per milliliter in each of the groups 5 weeks after tumor inoculation (* $P<0.05$ compared to Control group; # $P<0.05$ compared to one agent alone or two agent combination treatment groups). Data shown are representative of two independent experiments.

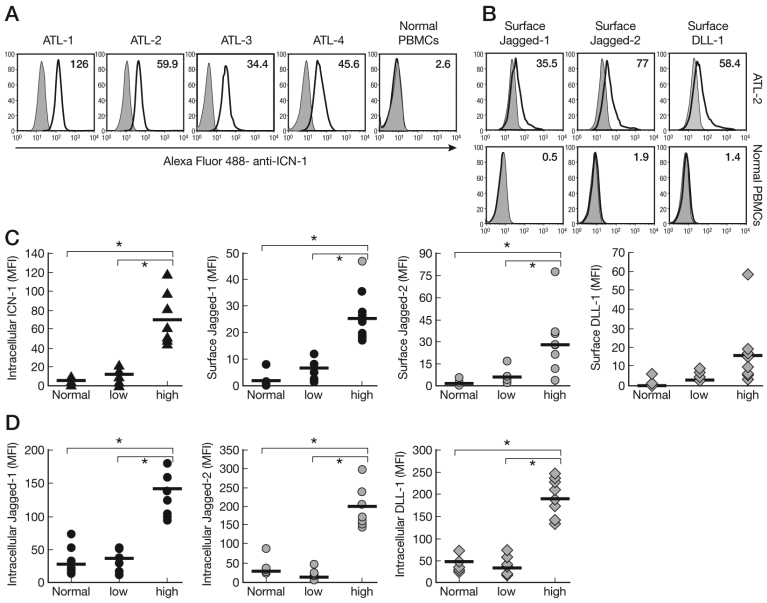

Figure 7. PBMCs from patients with chronic/ smoldering ATL had increased ICN-1 and upregulated expression of Notch-1 ligands

(A)Increased ICN-1 was detected in ATL leukemic ells when compared to unseparated $CD4^+$ T-cells from normal PBMCs. Gating on the $CD3^{low}CD4^{high}$ ATL cells of the patients, we demonstrated increased intracellular ICN-1 expression in leukemic cells within PBMCs from patients with chronic/smoldering ATL. Normal unseparated $CD4^+$ T-cells from PBMCs were used as the control. Filled grey histograms are isotype controls. (B) Patient ATL-2 had upregulated Notch-1 ligand expression on the surface of ATL cells. Gating on the $CD3^{low}CD4^{high}$ ATL cells of the patients, the surface expressions of Notch ligands---Jagged-1, Jagged-2, DLL-1 were increased in ATL-2 compared to those of normal PBMCs. Filled grey histograms are isotype controls. (C) Increased surface expression of Jagged-1 and Jagged-2 on ATL cells in ICN-1^{high} groups. Gating on the $CD3^{low}CD4^{high}$ ATL cells of the patients, surface expression of Notch ligands were detected by flow cytometry. Normal donors (Normal, N=10), ICN-1^{low} ATL group (low, N=6) and ICN-1^{high} ATL group (high, N=8) were detected by flow cytometry (* P<0.05). (D) Increased intracellular expression of Notch ligands was observed on ATL cells in the ICN-1^{high} groups. Gating on the $CD3^{low}CD4^{high}$ ATL cells of the patients, intracellular expression of Notch ligands were detected by flow cytometry. The ligands of normal donors (Normal, N=10), ICN-1^{low} ATL group (low, N=6) and ICN-1^{high} ATL group (high, N=8) were detected by flow cytometry(* P<0.05).

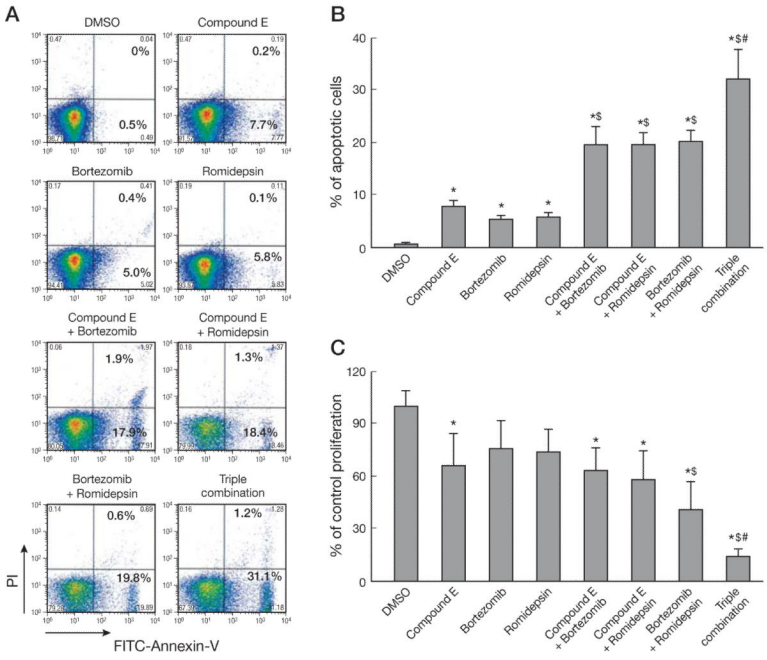

Figure 8. Ex vivo triple combination treatment induced significant apoptosis of PBMCs from chronic/smoldering ATL patients

(A) PBMCs from a patient were incubated with diverse agents (2μM Compound E, 2nM Bortezomib and 1nM Romidepsin) for 48 hours. Apoptosis detection was performed by Annexin V/PI staining and analyzed by flow cytometry. Annexin V^+/PI^- (lower right quadrant) areas stand for early apoptotic cells, and Annexin V^+/PI^+ (upper right quadrant) areas stand for late apoptotic or necrotic cells. (B) Bar graphs represent the percentages of early apoptotic cells (Annexin V^+/PI^-) after treatment with agents. Results are expressed as Mean ± SD (*P<0.05 compared to the DMSO group, $^{\$}$ P<0.05 compared to single agent treatment groups, $^{\#}P$<0.05 compared to two combination treatment groups). N=8. (C) The triple combination effectively suppressed spontaneous proliferation in certain chronic/smoldering ATL patients. The 6-day spontaneous proliferation of *ex vivo* PBMCs was assayed on cells from chronic/smoldering ATL patients by ^{3}H-TdR incorporation. Inhibitors were provided alone or in combination (2μM Compound E, 2nM Bortezomib and 1nM Romidepsin). In the presence of the triple combination the spontaneous proliferation was inhibited significantly (* P<0.01 compared with DMSO group, $^{\$}P$<0.05 compared to single agent treatment groups, $^{\#}P$<0.05 compared to two combination treatment groups). N=8.